Photon-tagged heavy meson production in high energy nuclear collisions

Zhong-Bo Kang and Ivan Vitev

Photon-tagged heavy meson production in high energy nuclear collisions

Zhong-Bo Kang[1, *] and Ivan Vitev[2, †]

[1]*RIKEN BNL Research Center, Brookhaven National Laboratory, Upton, NY 11973, USA*
[2]*Los Alamos National Laboratory, Theoretical Division, Los Alamos, NM 87545, USA*
(Dated: June 10, 2011)

We study the photon-triggered light and heavy meson production in both p+p and A+A collisions. We find that a parton energy loss approach that successfully describes inclusive hadron attenuation in nucleus-nucleus reactions at RHIC can simultaneously describe well the experimentally determined photon-triggered light hadron fragmentation functions. Using the same framework, we generalize our formalism to study photon-triggered heavy meson production. We find that the nuclear modification of photon-tagged heavy meson fragmentation functions in A+A collision is very different from that of the photon-tagged light hadron case. While photon-triggered light hadron fragmentation functions in A+A collisions are suppressed relative to p+p, photon-triggered heavy meson fragmentation functions can be either enhanced or suppressed, depending on the specific kinematic region. The anticipated smaller energy loss for b-quarks manifests itself as a flatter photon-triggered B-meson fragmentation function compared to that for the D-meson case. We make detailed predictions for both RHIC and LHC energies. We conclude that a comprehensive comparative study of both photon-tagged light and heavy meson production can provide new insights in the details of the jet quenching mechanism.

PACS numbers: 12.38.Bx, 24.85.+p, 25.75.Cj

I. INTRODUCTION

High transverse momentum partons and their hadronic fragments are powerful and valuable probes of the high energy density matter created at the Relativistic Heavy Ion Collider (RHIC) and the Large Hadron Collider (LHC). These energetic partons are created in the early stage of the collisions and therefore provide access to the space-time history of the transient hot and dense nuclear medium - the quark-gluon plasma (QGP) created in the heavy ion reactions. Specifically, as they propagate through the QGP, they interact with the medium and lose energy, a phenomenon known as "jet quenching" [1–8].

Experimentally, there has been tremendous progress in recent years [9] in establishing the jet quenching phenomenon from different observables, such as the suppression of single hadron production [10–12], dihadron correlations [13, 14], γ-hadron correlations [15, 16], and ultimately the alteration of inclusive jet [17] and dijet production [18, 19]. Theoretically, many perturbative QCD-based models of jet quenching have been developed and used to extract the medium properties [20], especially the QGP parton number and energy densities. They are able to successfully describe most of the experimental data and the measured nuclear modification factor R_{AA} of single hadron production in particular.

To study jet quenching and parton energy loss in more detail and thus constrain the medium properties better, more sophisticated observables have been proposed to improve our understanding of inelastic parton interactions in the QGP. One such example is γ-triggered hadron production and correlations [21]: one studies jet quenching by measuring the p_T distribution of charged hadrons in the opposite direction of a trigger direct photon. Since the photon does not interact with the dense medium, its energy approximately reflects that of the initial away-side parton before energy loss up to corrections at next-to-leading order in α_s. One can therefore study the effective medium modification of the jet fragmentation function. Earlier studies on the γ-triggered light hadron correlations [22–24] seem to be roughly compatible with the experimental data.

Although jet quenching has been successful in describing most of the experimental findings, there are still remaining puzzles. Resolving these puzzles will eventually uncover the exact underlying mechanism for the suppression of leading particles and jets. One well-known difficulty is related to the fact that the c and b-quark parton-level energy loss in the QGP has not been sufficient in the past to explain the large suppression of non-photonic $e^+ + e^-$ measured at RHIC [25, 26]. These non-photonic electrons come from the semileptonic decays of D and B mesons. In the framework of perturbative QCD, collisional dissociation of heavy-mesons in the QGP has been suggested as an

additional suppression mechanism [27, 28]. To distinguish with confidence between theoretical models one hopes to have a direct measurement of the heavy meson cross sections in both p+p and A+A collisions. Such direct measurements are finally becoming available from both RHIC and the LHC experiments.

The main goal of this paper is to investigate new experimental observables, such as γ-triggered hadron production, and make simultaneous predictions for both light and heavy meson final states. Naturally, we will first focus on the standard parton energy loss mechanism in the QGP. More specifically, we present detailed studies of both γ-triggered away-side light hadron and heavy meson spectra in heavy ion collisions. Within the same energy loss formalism - the Gyulassy-Levai-Vitev (GLV) approach - we study how the QGP medium affects the γ-triggered light and heavy meson effective fragmentation functions. We find that the nuclear modification factor I_{AA} behaves very differently depending on the parent parton mass: I_{AA} is considerably suppressed for light hadrons ($I_{AA} < 1$), whereas it can be suppressed ($I_{AA} < 1$) or enhanced ($I_{AA} > 1$) for heavy mesons, depending on the kinematic region, due to the different shape of the heavy quark fragmentation functions. Furthermore, we find that the nuclear modification I_{AA} is flatter in the B-meson case compared to that of D-mesons due to the smaller energy loss for b-quarks in the non-asymptotic (finite energy) case. Thus, a comparative study of γ-triggered light and heavy meson correlations can be a very useful probe of the physics that underlays the experimentally established jet quenching.

The rest of our paper is organized as follows: in Sec. II we present the relevant formalism for both photon-tagged light hadron and heavy meson production. In Sec. III we present our phenomenological studies. We first compare our calculation to the experimental data on photon+light hadron correlations. Then, we make predictions for photon-triggered light and heavy meson production relevant to both RHIC and LHC experiments and discuss the differences in the observed nuclear modification. We conclude our paper in Sec. IV.

II.   PHOTON-TAGGED LIGHT AND HEAVY MESON PRODUCTION

In this section we present the relevant formalism for the photon-triggered light and heavy meson production in nucleon-nucleon collisions. These formula will then be used in the phenomenological studies in the next section.

A.   Photon-tagged light hadron production

Within the framework of the collinear perturbative QCD factorization approach, the lowest order (LO) differential cross section for back-to-back photon-light-hadron production can be obtained from the partonic processes: $q\bar{q} \to \gamma g$ and $qg \to \gamma q$ and is given by [29]

$$\frac{d\sigma_{NN}^{\gamma h}}{dy_\gamma dy_h dp_{T_\gamma} dp_{T_h}} = \frac{2\pi\alpha_{em}\alpha_s}{S^2} \sum_{a,b,c} D_{h/c}(z_T) \frac{f_{a/N}(x_a)f_{b/N}(x_b)}{x_a x_b} \overline{|M|}^2_{ab\to\gamma c}, \tag{1}$$

where S is the squared center of mass energy of the hadronic collisions, and z_T, x_a, and x_b are given by

$$z_T = \frac{p_{T_h}}{p_{T_\gamma}}, \qquad x_a = \frac{p_{T_\gamma}}{\sqrt{S}}\left(e^{y_\gamma} + e^{y_h}\right), \qquad x_b = \frac{p_{T_\gamma}}{\sqrt{S}}\left(e^{-y_\gamma} + e^{-y_h}\right). \tag{2}$$

Here, y_γ and p_{T_γ} (y_h and p_{T_h}) are the rapidity and transverse momentum of the photon (away-side hadron), respectively. We denote by $f_{a,b/N}(x_{a,b})$ the distribution functions of partons a,b in the nucleon and $D_{h/c}(z)$ is the fragmentation function of parton c into hadron h. $\overline{|M|}^2_{ab\to\gamma c}$ are the squared matrix elements for $ab \to \gamma c$ partonic processes, and are given by

$$\overline{|M|}^2_{qg\to\gamma q} = e_q^2 \frac{1}{N_c}\left[-\frac{s}{t} - \frac{t}{s}\right], \qquad \overline{|M|}^2_{gq\to\gamma q} = e_q^2 \frac{1}{N_c}\left[-\frac{s}{u} - \frac{u}{s}\right], \tag{3}$$

$$\overline{|M|}^2_{q\bar{q}\to\gamma g} = \overline{|M|}^2_{\bar{q}q\to\gamma g} = e_q^2 \frac{N_c^2 - 1}{N_c^2}\left[\frac{t}{u} + \frac{u}{t}\right], \tag{4}$$

where s, t, u are the partonic Mandelstam variables, e_q is the fractional electric charge of the light quark, and $N_c = 3$ is the number of colors.

Experimentally, one typically defines the so-called γ-triggered fragmentation function

$$D_{NN}^{\gamma h}(z_T) = \frac{\int dy_\gamma dy_h dp_{T_\gamma} p_{T_\gamma} \frac{d\sigma_{NN}^{\gamma h}}{dy_\gamma dy_h dp_{T_\gamma} dp_{T_h}}}{\int dy_\gamma dp_{T_\gamma} \frac{d\sigma_{NN}^{\gamma}}{dy_\gamma dp_{T_\gamma}}} \tag{5}$$

for nucleon-nucleon collisions and a similar $D_{AA}^{\gamma h}(z_T)$ per binary scattering for A+A collisions. The denominator defines the normalization and is given by

$$\frac{d\sigma_{NN}^{\gamma}}{dy_\gamma dp_{T_\gamma}} = \sum_h \int dy_h dp_{T_h} \frac{d\sigma_{NN}^{\gamma h}}{dy_\gamma dy_h dp_{T_\gamma} dp_{T_h}}, \tag{6}$$

which is just the cross section for direct photon production. To quantify the modification of γ-triggered fragmentation function in A+A collisions relative to that in nucleon-nucleon collisions due to the jet quenching, one introduces the nuclear modification factor,

$$I_{AA}^{\gamma h}(z_T) = \frac{D_{AA}^{\gamma h}(z_T)}{D_{NN}^{\gamma h}(z_T)}. \tag{7}$$

Note that, in spite of their suggestive name, γ-triggered fragmentation functions are derived from the observed away-side meson distribution and thus reflect all input in a pQCD calculation - the parton distributions, the hard scattering cross sections, the medium-induced radiative correction (or parton energy loss) and the parton decay probabilities - not only the fragmentation process itself.

B.   Photon-tagged heavy meson production

Within the perturbative QCD factorization approach there have been different ways to calculate heavy quark production. One of them is called a fixed-flavor-number scheme (FFNS) [30–32] and is based on the assumption that the gluon and the three light quarks (u, d, s) are the only active partons. The heavy quark appears only in the final state and is produced in the hard scattering process of light partons. The heavy quark mass m is explicitly retained throughout the calculation. The other approach is called a variable-flavor-number scheme (VFNS) [33–35] and describes the heavy quark as a massless parton of density $f_{Q/N}(x, \mu^2)$ in the nucleon, with the boundary condition $f_{Q/N}(x, \mu^2) = 0$ for $\mu \leq m$. Thus, the heavy quark mass m is set to zero in the short-distant partonic cross section[1].

In this paper, we are particularly interested in studying the jet quenching effects for both light and heavy mesons. The different amount of energy loss during quark propagation in the medium created in heavy ion collisions is due to the mass difference between light and heavy quarks, at least in perturbative QCD. With this in mind, we want to keep explicitly the heavy quark mass in our calculation. In other words, we favor the FFNS scheme for the project at hand. Within this scheme, the photon-tagged heavy mesons are produced through the following partonic processes - (a) quark-antiquark annihilation: $q\bar{q} \to Q\bar{Q}\gamma$; (b) gluon-gluon fusion: $gg \to Q\bar{Q}\gamma$. The sample Feynman diagrams are given in Fig. 1. It is important to realize that in the FFNS scheme photon+heavy quark events are generated to LO by the $2 \to 3$ processes, to be compared to the usual $2 \to 2$ processes for the photon+light hadron events at LO.
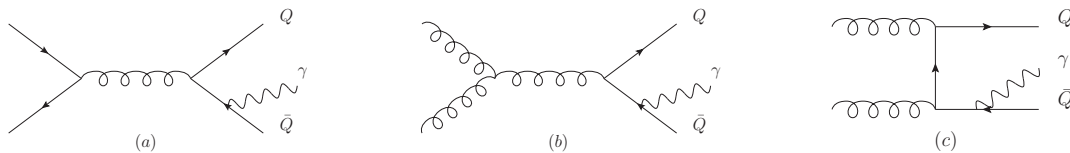

FIG. 1. Sample Feynman diagrams at leading order for direct photon plus heavy quark production: (a) for light quark-antiquark annihilation $q\bar{q} \to Q\bar{Q}\gamma$, (b) and (c) for gluon-gluon fusion $gg \to Q\bar{Q}\gamma$.

The differential cross section for photon-tagged heavy meson production takes the following form [32]:

$$\frac{d\sigma_{NN}^{\gamma H}}{dy_\gamma dy_h dp_{T_\gamma} dp_{T_H}} = \frac{\alpha_{em}\alpha_s^2}{2\pi S} \sum_{ab} \int \frac{dz}{z^2} D_{H/Q}(z) \int \frac{dx_a}{x_a} f_{a/N}(x_a) \int d\phi \frac{1}{x_b} f_{b/N}(x_b)$$

$$\times \frac{p_{T_\gamma} p_{T_H}}{x_a S - \sqrt{S}(p_{T_\gamma} e^{y_\gamma} + m_{T_Q} e^{y_H})} \overline{|M|}_{ab \to Q\bar{Q}\gamma}, \tag{8}$$

where $D_{H/Q}(z)$ is the heavy quark Q to heavy meson H fragmentation function and $\phi = \phi_h - \phi_\gamma \in [\pi/2, 3\pi/2]$ is the azimuthal angle between the triggered photon and the associated heavy meson on the away side. We denote by

---

$m_{T_Q} = \sqrt{p_{T_Q}^2 + m^2}$ the transverse mass and by $p_{T_Q} = p_{T_H}/z$ the transverse momentum for the heavy quark. The parton momentum fraction x_b is fixed by the kinematics and has the following form

$$x_b = \frac{x_a\sqrt{S}(p_{T_\gamma}e^{-y_\gamma} + m_{T_Q}e^{-y_H}) + 2p_{T_\gamma}p_{T_Q}\cos\phi - p_{T_\gamma}m_{T_Q}(e^{y_\gamma - y_H} + e^{y_H - y_\gamma})}{x_a S - \sqrt{S}(p_{T_\gamma}e^{y_\gamma} + m_{T_Q}e^{y_H})}. \tag{9}$$

The partonic matrix elements $\overline{|M|}_{ab \to Q\bar{Q}\gamma}$ can be calculated in perturbative QCD. Note that the cross section does not produce any singularity since the heavy quarks have been taken to be massive explicitly. Therefore no regularization is needed despite the fact that we are actually dealing with a $2 \to 3$ process. The cross section for photoproduction of heavy quarks has been published in [36]. By using crossing symmetry, we can infer the spin-averaged matrix elements in our case. We list the results here for completeness. For the quark-antiquark annihilation channel $q(p_1) + \bar{q}(p_2) \to Q(p_3) + \bar{Q}(p_4) + \gamma(p_5)$ we have

$$\overline{|M|}_{q\bar{q} \to Q\bar{Q}\gamma}^2 = \frac{N_c^2 - 1}{N_c^2}\left[e_Q^2 A_1 + e_q^2 A_2 + e_Q e_q A_3\right], \tag{10}$$

where e_Q is the fractional electric charge of the heavy quark, and the coefficients A_1, A_2, and A_3 are given by

$$A_1 = \frac{\left(p_{24}^2 + p_{23}^2 + p_{14}^2 + p_{13}^2 + m^2 s_{34}\right)p_{34}}{p_{45}p_{35}p_{12}s_{34}} + \frac{m^2\left(p_{25}^2 + p_{15}^2\right)}{2p_{12}^2 p_{45}p_{35}}$$
$$+ \frac{m^2\left(p_{24}^2 + p_{14}^2 + p_{23}^2 + p_{13}^2 - p_{12}s_{34}\right)}{p_{12}^2 s_{34}}\left[\frac{1}{p_{45}} + \frac{1}{p_{35}}\right]$$
$$- \frac{m^2}{2p_{12}^2}\left[\frac{p_{24}^2 + p_{14}^2 + m^2 p_{12}}{p_{35}^2} + \frac{p_{23}^2 + p_{13}^2 + m^2 p_{12}}{p_{45}^2}\right], \tag{11}$$

$$A_2 = \frac{p_{24}^2 + p_{23}^2 + p_{14}^2 + p_{13}^2 + 2m^2 p_{12}}{p_{25}p_{15}s_{34}} + \frac{2m^2\left(p_{25}^2 + p_{15}^2\right)}{p_{25}p_{15}s_{34}^2}, \tag{12}$$

$$A_3 = \frac{p_{24}^2 + p_{23}^2 + p_{14}^2 + p_{13}^2 + m^2(p_{12} + \frac{1}{2}s_{34})}{p_{12}s_{34}}\left[\frac{p_{24}}{p_{45}p_{25}} + \frac{p_{13}}{p_{35}p_{15}} - \frac{p_{14}}{p_{45}p_{15}} - \frac{p_{23}}{p_{35}p_{25}}\right]$$
$$+ \frac{2m^2}{p_{12}s_{34}}\left[\frac{p_{13} - p_{23}}{p_{45}} + \frac{p_{24} - p_{14}}{p_{35}}\right]. \tag{13}$$

Here, we have used the notation $p_{ij} = p_i \cdot p_j$, $s_{34} = (p_3 + p_4)^2$. For the gluon-gluon fusion channel $g(p_1) + g(p_2) \to Q(p_3) + \bar{Q}(p_4) + \gamma(p_5)$ we have

$$\overline{|M|}_{gg \to Q\bar{Q}\gamma}^2 = -\frac{1}{N_c(N_c^2 - 1)}e_Q^2\left[(R_{QED} + 11 \text{ perm's}) + N_c^2\left(R_{KF} + 3 \text{ perm's}\right)\right]. \tag{14}$$

The R_{QED} has to be summed over 12 permutations corresponding to the 6 permutations of the momenta p_1, p_2, $-p_5$ and two permutations of the momenta p_3 and p_4. R_{KF} has to be summed over 4 permutations corresponding to the interchange of p_1, p_2 and p_3, p_4. One such expression for R_{QED} is given by

$$R_{QED} = \frac{s_{34}p_{24}^2}{8p_{14}p_{13}p_{45}p_{35}}$$
$$- \frac{m^2}{2p_{35}}\left[\frac{1}{p_{14}}\left(\frac{s_{34}}{2p_{13}} - \frac{p_{23}}{p_{14}} + 3\right) + \frac{p_{45} - p_{23} + p_{14}}{2p_{24}p_{13}} - \frac{1}{p_{45}} - \frac{3}{2p_{13}}\right]$$
$$- \frac{m^4}{2p_{35}p_{14}}\left[\frac{1}{2p_{13}}\left(\frac{p_{13} - 3p_{14} + 2p_{45}}{p_{24}} + \frac{3p_{24}}{p_{45}} - 4\right) + \frac{2}{p_{35}}\right]$$
$$+ \frac{m^6}{p_{35}p_{14}}\left[\frac{1}{2p_{13}}\left(\frac{1}{2p_{45}} - \frac{1}{p_{24}}\right) + \frac{1}{2p_{14}}\left(\frac{1}{2p_{35}} - \frac{1}{p_{23}}\right)\right], \tag{15}$$

and R_{KF} is given by

$$
\begin{aligned}
R_{KF} = &-\frac{1}{2p_{12}}\left[\frac{p_{45}^2}{p_{13}p_{24}} + \frac{p_{14}^2}{p_{45}p_{35}}\left(\frac{p_{14}}{p_{24}} + \frac{p_{13}}{p_{23}}\right)\right] \\
&+\frac{m^2}{2p_{12}^2}\left[1 - \frac{2p_{14}}{p_{35}}\left(\frac{p_{14}}{p_{35}} + \frac{p_{23}}{p_{45}}\right)\right] + \frac{m^2}{4p_{14}p_{23}}\left[-\frac{2p_{45}}{p_{23}} + \frac{2(p_{45}+p_{35})}{p_{12}} - 7\right] \\
&+\frac{m^2}{2p_{35}p_{14}}\left[\frac{p_{45}-p_{12}}{p_{23}} + \frac{p_{23}-p_{12}}{p_{45}} - \frac{p_{23}}{p_{14}} + \frac{p_{12}}{p_{35}} + 7\right] \\
&+\frac{m^2}{p_{35}}\left[\frac{1}{p_{12}}\left(\frac{p_{14}-p_{45}}{p_{23}} + \frac{2p_{14}}{p_{35}} + \frac{2p_{14}}{p_{45}} - 2\right) - \frac{1}{p_{45}} - \frac{3}{2p_{35}}\right] \\
&+\frac{m^4}{p_{35}p_{23}}\left[\frac{1}{p_{12}}\left(\frac{p_{45}}{p_{14}} + \frac{p_{14}}{p_{45}}\right) + \frac{1}{2p_{45}}\left(\frac{p_{12}}{p_{14}} + 2\right)\right] \\
&+\frac{m^4}{p_{35}}\left[\frac{1}{p_{12}}\left(-\frac{1}{p_{23}} - \frac{1}{p_{35}} + \frac{1}{p_{14}} - \frac{2}{p_{45}}\right) - \frac{1}{p_{14}}\left(\frac{1}{p_{14}} - \frac{1}{p_{35}} + \frac{2}{p_{23}}\right)\right] \\
&+\frac{m^4}{p_{14}p_{23}}\left(\frac{1}{2p_{12}} + \frac{1}{p_{14}}\right) - \frac{m^6}{p_{14}^2}\left[\left(\frac{1}{2p_{35}} + \frac{p_{14}}{2p_{23}p_{45}}\right)^2 + \frac{1}{p_{23}}\left(\frac{1}{4p_{23}} - \frac{1}{p_{35}}\right)\right].
\end{aligned}
\tag{16}
$$

With the cross sections at hand, the experimentally accessible γ-triggered heavy meson fragmentation function is defined as

$$
D_{NN}^{\gamma H}(z_T) = \frac{\int dy_\gamma dy_H dp_{T_\gamma} p_{T_\gamma} \frac{d\sigma_{NN}^{\gamma H}}{dy_\gamma dy_H dp_{T_\gamma} dp_{T_H}}}{\int dy_\gamma dp_{T_\gamma} \frac{d\sigma_{NN}^{\gamma Q}}{dy_\gamma dp_{T_\gamma}}},
\tag{17}
$$

where the denominator is the differential cross section of photon and heavy meson production summed over all the heavy mesons

$$
\frac{d\sigma_{NN}^{\gamma Q}}{dy_\gamma dp_{T_\gamma}} = \sum_H \int dy_H dp_{T_H} \frac{d\sigma_{NN}^{\gamma H}}{dy_\gamma dy_H dp_{T_\gamma} dp_{T_H}}.
\tag{18}
$$

It can be written as

$$
\begin{aligned}
\frac{d\sigma_{NN}^{\gamma Q}}{dy_\gamma dp_{T_\gamma}} = &\frac{\alpha_{em}\alpha_s^2}{2\pi S}\sum_{ab}\int dy_Q dp_{T_Q}\int\frac{dx_a}{x_a}f_{a/N}(x_a)\int d\phi\frac{1}{x_b}f_{b/N}(x_b) \\
&\times\frac{p_{T_\gamma} p_{T_Q}}{x_a S - \sqrt{S}(p_{T_\gamma}e^{y_\gamma} + m_{T_Q}e^{y_Q})}\overline{|M|}_{ab\to Q\bar{Q}\gamma},
\end{aligned}
\tag{19}
$$

which is just part of the inclusive photon production cross section that has $\gamma + Q$ events.

Likewise, we can define a γ-triggered heavy meson fragmentation function $D_{AA}^{\gamma H}(z_T)$ in A+A collisions and the nuclear modification factor $I_{AA}^{\gamma H}(z_T) = D_{AA}^{\gamma H}(z_T)/D_{NN}^{\gamma H}(z_T)$. In the next section we will study how these fragmentation functions behave in both p+p and A+A collisions and, most importantly, how they are modified in A+A collisions due to jet quenching.

III.   PHENOMENOLOGICAL STUDIES IN P+P AND A+A COLLISIONS

In this section we will study the γ-triggered light hadron and heavy meson production in both p+p and A+A collisions. Final-state medium-induced radiative corrections are process dependent - they depend on the parameters of the QGP medium and, consequently, on the details of the heavy ion collision. However, in QCD they factorize from the hard scattering cross section [8] and enter the physical observables as a standard integral convolution. From the point of view of phenomenological applications, it is convenient to change the order of integration and include parton energy loss as an effective replacement of the fragmentation function $D_{h/c}(z)$ [37]:

$$
D_{h/c}(z) \Rightarrow \int_0^{1-z} d\epsilon\, P(\epsilon)\frac{1}{1-\epsilon}D_{h/c}\left(\frac{z}{1-\epsilon}\right).
\tag{20}
$$

Here, $P(\epsilon)$ is the probability distribution for a parton to lose a fraction of its energy $\epsilon = \sum_i \frac{\Delta E_i}{E}$ due to multiple gluon emission. In our calculation $P(\epsilon)$ is obtained using the GLV formalism for evaluating the medium-induced gluon bremsstrahlung [38, 39] and the Poisson approximation. Note that it is not mandatory to employ Eq. (20) in jet quenching phenomenology. One can alternatively evaluate the attenuated partonic cross section prior to fragmentation and obtain identical results [28].

We take into account parton energy loss in γ-hadron correlation in high energy heavy-ion collisions as in Eq. (20) for simplicity. We do not perform a new evaluation of the energy loss since we aim at a direct and consistent comparison between different final states in the same jet quenching formalism. Instead, we employ the differential medium-induced bremsstrahlung distributions and energy loss probabilities $P(\epsilon)$ for light partons and heavy quarks obtained in [28, 40]. An illustration of these probabilities

$$\int_0^1 P(\epsilon)d\epsilon = 1, \qquad \int_0^1 \epsilon\, P(\epsilon)d\epsilon = \left\langle \frac{\Delta E}{E} \right\rangle, \qquad \epsilon = \sum_i \frac{\Delta E_i}{E} \tag{21}$$

is given in Fig. 2. Note that, in the probabilistic application of parton energy loss, larger $\langle \Delta E/E \rangle$ corresponds to a distribution skewed toward large ϵ and smaller $\langle \Delta E/E \rangle$ corresponds to a distribution skewed toward small ϵ. All results include an average over the jet production points distributed according to the binary collision density in an optical Glauber model. These energetic jets propagate through the Bjorken expanding medium that follows the number of participants density [28, 40]. The left panel of Fig. 2 corresponds to central Au+Au collisions at RHIC and parton energy $E = 10$ GeV and the right panel of Fig. 2 corresponds to central Pb+Pb collisions at the LHC and parton energy $E = 25$ GeV.

The difference between light quarks and gluons arises from the quadratic Casimir, or average squared color charge, of the parton. Note that the naive relation $\langle \Delta E \rangle_g = C_A/C_F \langle \Delta E \rangle_q$ is approximately fulfilled only if $\langle \Delta E \rangle_{q,g} \ll E$. In the realistic case, $\langle \Delta E \rangle_g < C_A/C_F \langle \Delta E \rangle_q$ and the deviation form the naive scaling can be significant. On the other hand, the difference between light and heavy quarks is related to the quark mass [25, 26, 39]. In the very high energy limit, for coherent medium-induced bremsstrahlung, the mass dependence of parton energy loss disappears. The calculations that we present in this paper are not in this asymptotic limit. Furthermore, for partons of effective mass $gT \sim m_c$, where g is the coupling constant and T is the temperature of the quark-gluon plasma created in heavy ion collisions, there is very little difference between the light quarks and the charm quarks. This is clearly seen in both panels of Fig. 2 and well understood. For the much heavier bottom quarks $m_b \gg m_c \sim gT$, however, the energy loss is noticeably smaller and $P(\epsilon)$ is skewed toward smaller values of ϵ.
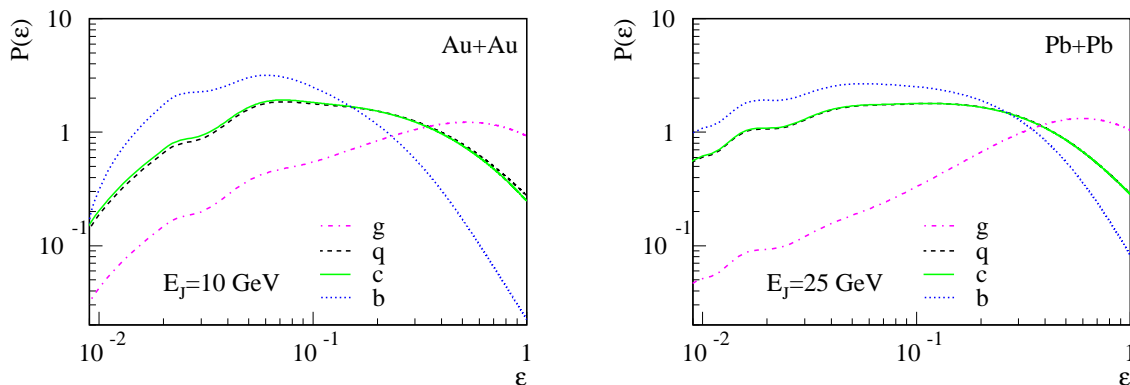

FIG. 2. The probability distribution $P(\epsilon)$ for partons to lose a fraction ϵ of their energy is shown for gluons (dot-dashed), light quarks (dashed), charm quarks (solid) and bottom quarks (dotted). Left panel: central Au+Au collisions at RHIC and parton energy $E_J = 10$ GeV. Right panel: central Pb+Pb collisions at the LHC and parton energy $E_J = 25$ GeV.

A. Comparison to experimental data: γ-triggered light hadron production

In this subsection we will compare our calculations for γ-triggered light hadron production to the experimental data at RHIC. We will use CTEQ6 parton distribution function [41] and deFlorian-Sassot-Stratmann (DSS) light hadron fragmentation function [42].

In Fig. 3 (left and top right panels) we show our results compared to both PHENIX [15] and STAR data [16]. For p+p collisions we use the definition given in Eq. (5). As seen from these figures, the perturbative QCD calculation gives

a very good descriptions of the experimental data. For Au+Au collisions we use the same energy loss distributions that were used to describe single hadron suppression. As can be seen from Fig. 3, the calculated $D_{AA}^{\gamma h}(z_T)$ are in good agreement with the experimental data with the possible exception of the large $z_T \to 1$ region in the STAR data. This part of phase space is also inherently difficult to measure accurately. Such agreement gives an independent confirmation of the jet quenching mechanism in light hadron production.
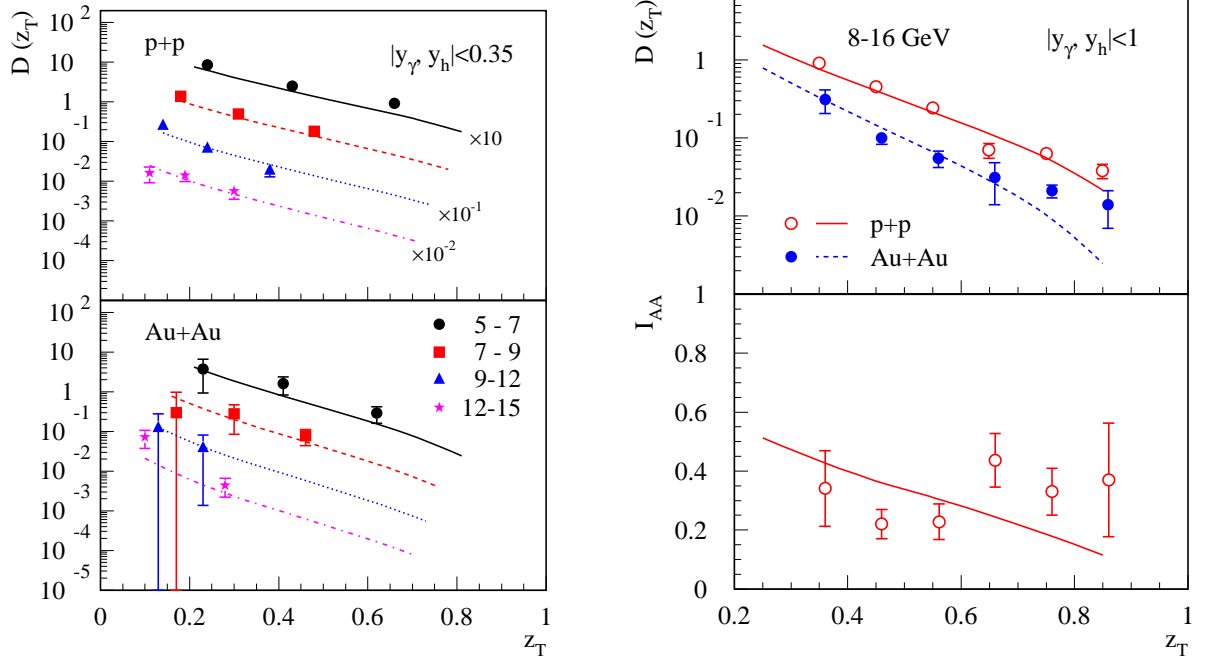

FIG. 3. γ-triggered fragmentation functions $D(z_T)$ (left) and (top right) are plotted as a function of z_T at $\sqrt{S_{NN}} = 200$ GeV. Left: top for p+p collisions, bottom for Au+Au collisions. Photon and hadron rapidities are integrated over $[-0.35, 0.35]$, while the trigger particle (the photon) momentum has been integrated over $[5, 7]$, $[7, 9]$, $[9, 12]$, and $[12, 15]$ GeV from top to bottom. Data is from PHENIX [15]. Right: top for $D(z_T)$ - solid for p+p collision, and dashed for Au+Au collision; bottom for nuclear modification factor I_{AA}. The photon and hadron rapidities are integrated over $[-1, 1]$, and the photon momentum is integrated over $[8, 16]$ GeV. Data is from STAR [16].
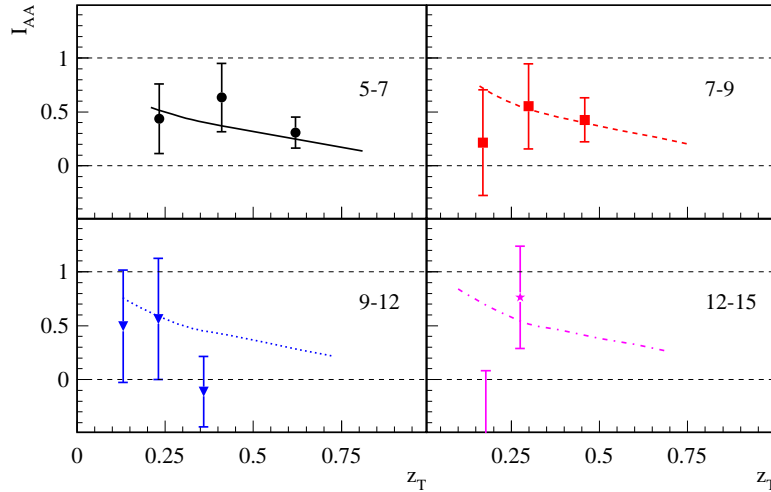

FIG. 4. Nuclear modification factor $I_{AA}(z_T)$ is plotted as a function of z_T at $\sqrt{S_{NN}} = 200$ GeV. The numbers on the right top corner in each plots are the range of the photon momentum, while the photon and hadron rapidities are integrated over $[-0.35, 0.35]$. The data is from PHENIX [15].

It is worthwhile to point out that the γ-triggered light hadron fragmentation function $D_{AA}^{\gamma h}(z_T)$ in Au+Au collisions

is suppresses relative to that in p+p collisions. This is understandable since at LO $D^{\gamma h}(z_T) \propto D_{h/c}(z_T)$ according to Eq. (1), where $D_{h/c}(z)$ is a fast falling function of z. Since jet quenching can effectively be thought of as a mechanism that probes slightly higher z as in $D_{h/c}(\frac{z}{1-\epsilon})$ according to Eq. (20), sampling higher z leads to a smaller fragmentation function. Thus, the γ-triggered fragmentation function in A+A collisions will be suppressed compared to p+p collisions. We will find this behavior can be altered in the γ-triggered heavy meson production as we will demonstrate below.

In Fig. 3 (bottom right panel) and Fig. 4, we compare our calculations of $I_{AA}^{\gamma h}$ to the experimental data. Being a ratio of the γ-triggered fragmentation functions in A+A and p+p collisions, the nuclear modification factor $I_{AA}^{\gamma h}(z_T) = D_{AA}^{\gamma h}(z_T)/D_{pp}^{\gamma h}(z_T)$ has much larger error bars. Our results are consistent with the experimental data (within the error bars).

B. Predictions for γ-triggered light and heavy meson production

In this subsection we will make predictions for the γ-triggered light and heavy meson production at both RHIC and LHC energies and will compare the different features of the in-medium modification depending on the parton mass. We use D and B-meson fragmentation functions as calculated in [28] and choose $m = 1.3$ (4.5) GeV for the charm (bottom) quarks. For γ-triggered heavy meson production we have integrated over the relative azimuthal angle $\phi = \phi_h - \phi_\gamma$ in the region: $|\phi - \pi| < \pi/5$ in Eq. (8), following the experimentally applied cuts [15, 16].
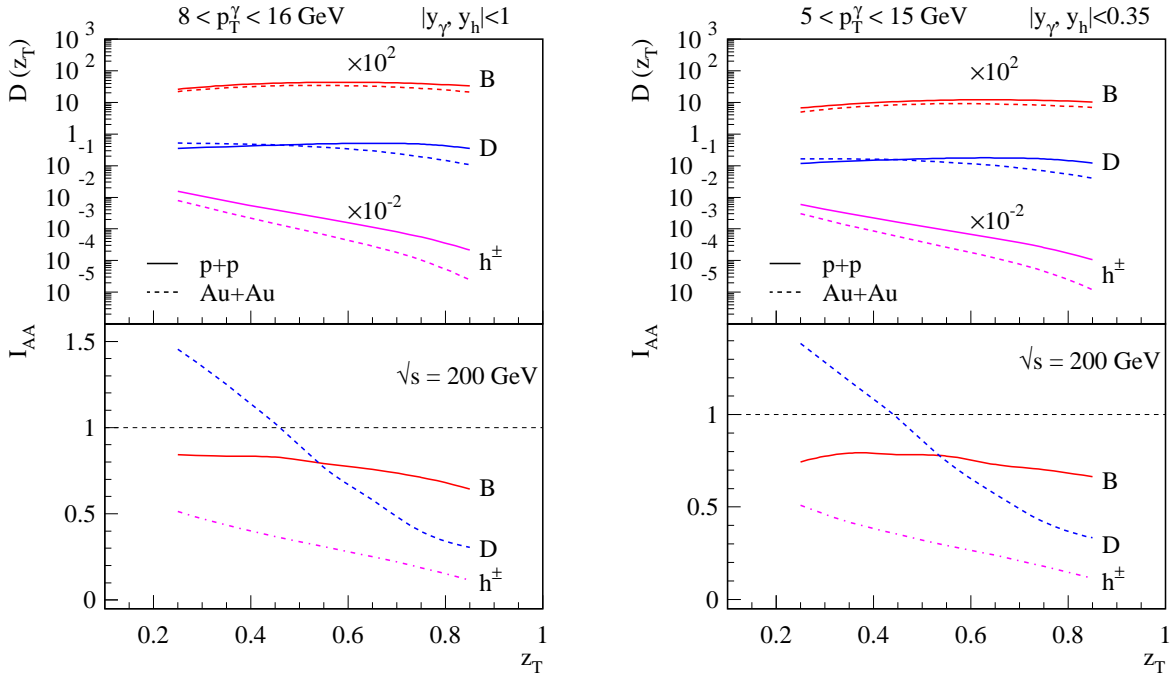

FIG. 5. Top panels: predictions for γ-triggered fragmentation functions $D(z_T)$ where the solid lines are for p+p collisions and the dashed lines are for central Au+Au collisions. Bottom panels: predictions for the nuclear modification factor $I_{AA}(z_T)$ where the solid lines are for B-meson, the dashed lines are for D-meson, and the dash-dotted lines are for charged hadrons. The left plot has kinematics similar to STAR, while the right plot has kinematics similar to PHENIX.

In the upper panels of Fig. 5 we plot $D(z_T)$ as a function of z_T at $\sqrt{S_{NN}} = 200$ GeV for both p+p and central Au+Au collisions. Left panels reflect STAR kinematics and right panels reflect PHENIX kinematics. As seen clearly in the plots, $D(z_T)$ for light hadrons and heavy mesons are very different. For light hadrons, the γ-triggered fragmentation function $D^{\gamma h}(z_T)$ drops very fast as z_T increases, consistent with the behavior of light hadron fragmentation function $D_{h/c}(z)$. On the other hand, the γ-triggered heavy meson fragmentation function $D^{\gamma H}(z_T)$ is a relatively flat function of z_T. Even though in the FFNS scheme $D^{\gamma H}(z_T)$ does not directly correspond to the heavy quark to heavy meson decay probability $D_{H/Q}(z)$ itself, it does reflect to some extent the major feature of the heavy meson fragmentation function: it grows at lower z and decreases at higher z. This difference in the fragmentation functions will lead to distinctive difference in the nuclear modification factor I_{AA} between light hadron and heavy meson.

In the bottom panels of Fig. 5 we plot $I_{AA}(z_T)$ as a function of z_T at RHIC for γ-triggered light charged hadrons
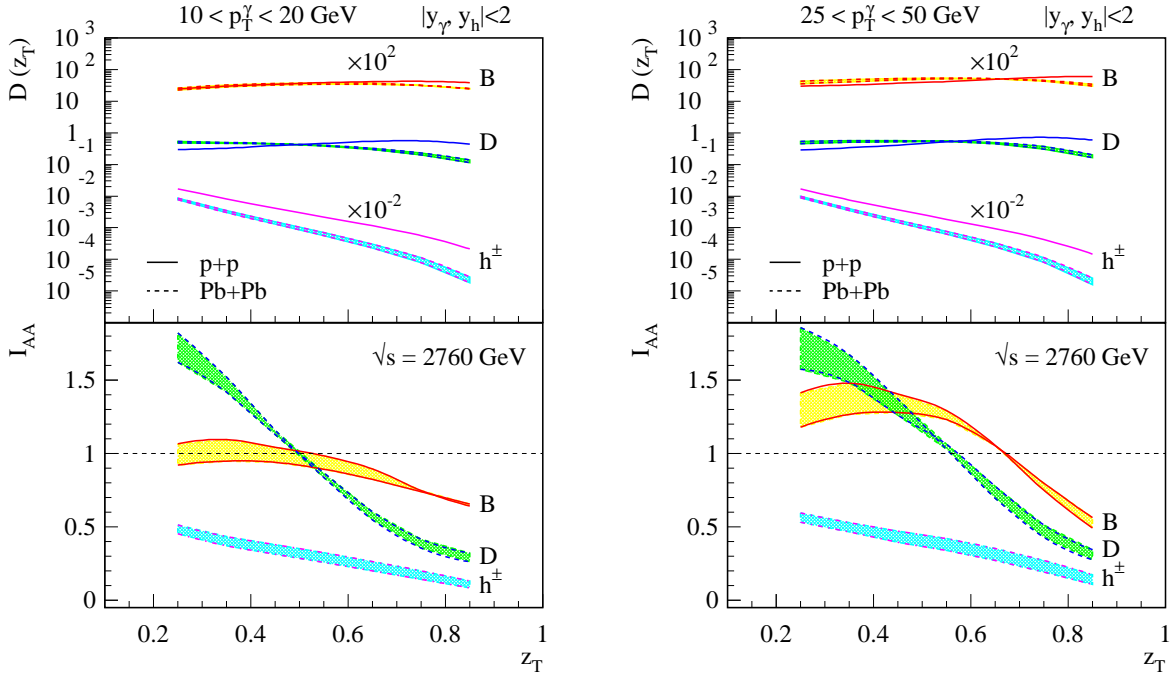
FIG. 6. Top panels: predictions for the γ-triggered fragmentation functions $D(z_T)$, where the solid lines are for p+p collisions and the dashed lines are for central Pb+Pb collisions at $\sqrt{S_{NN}} = 2.76$ TeV. Bottom panels: predictions for the nuclear modification factor $I_{AA}(z_T)$, where the solid lines are for B-meson, the dashed lines are for D-meson, and the dash-dotted lines are for charged hadrons. We have integrated the photon and hadron rapidities over $[-2, 2]$. For the left plot, the photon momentum is integrated over $[10, 20]$ GeV, while for the right plot, it has been integrated over $[25, 50]$ GeV.

(dot-dashed), D-mesons (dashed) and B-mesons (solid), respectively. They exhibit very different behavior. For light hadrons, one expects $I_{AA}^{\gamma h} < 1$ due to jet quenching, as explained above. The magnitude of this suppression arrises mainly from the steepness of the light hadron fragmentation function $D_{h/c}(z)$. On the other hand, according to Eq. (8), for the γ-triggered heavy meson case $I_{AA}^{\gamma H}$ really depends on the whole z-integration of the heavy meson fragmentation function $D_{H/Q}(z)$. If the integral is dominated by the small-z region, where $D_{H/Q}(z)$ grows with increasing z, jet quenching in Eq. (20) means sampling relatively larger-z and thus larger $D_{H/Q}(z)$. Consequently, one will then have $I_{AA}^{\gamma H} > 1$. On the other hand, if the integral is dominated by the large-z region, where $D_{H/Q}(z)$ decreases with increasing z, sampling relatively higher-z means smaller $D_{H/Q}(z)$. One thus has $I_{AA}^{\gamma H} < 1$.

One keeps in mind that we have three-particle final state, thus $z_T = p_{T_H}/p_{T_\gamma}$ is not the same as the momentum fraction z in heavy meson decay probability $D_{H/Q}(z)$ according to Eq. (8). Nevertheless, we find that the average $\langle z \rangle$ in the collision does increase as z_T increases. Thus, at high z_T where the z-integral in $I_{AA}^{\gamma H}$ is dominated by the large z region, one should expect that both B and D-mesons are suppressed due to jet quenching. The magnitude of the suppression should follow $I_{AA}^{\gamma B} > I_{AA}^{\gamma D} > I_{AA}^{\gamma h^\pm}$ if the heavy quark loses less energy than the light quark, as predicted by perturbative QCD calculations. On the other hand, in the low z_T region, according to our calculation, we find that $I_{AA}^{\gamma D} > 1$ for D-meson, consistent with our naive expectation, that is the low z region dominates the z integral in Eq. (8).

However, for γ-triggered B-mesons $I_{AA}^{\gamma B} < 1$ for the whole z_T region for the kinematics we have chosen at RHIC. This is due to the fact that our B-meson fragmentation function is even harder than the D-meson fragmentation function. It drops very fast at high z while increases only slowly at low z. Thus the nuclear modification from high z (suppression) wins over that from low z (enhancement) for the kinematic region we have chosen. Combining the analysis for both the low and the high z_T ends, one immediately finds that the nuclear modification $I_{AA}^{\gamma H}$ for γ-triggered B-meson fragmentation function is flatter than that for D-meson case. Another important reason for this flatter behavior and the smaller size of the nuclear modification is the smaller energy loss of b-quark in comparison to c-quark. Thus, the shape of the nuclear modification for the γ-triggered fragmentation functions can cary valuable information about the properties of medium-induced gluon bremsstrahlung.

In Fig. 6 we give predictions for the γ-triggered light and heavy meson production in both p+p and central Pb+Pb collisions at $\sqrt{S_{NN}} = 2.76$ TeV at the LHC. We integrate over both the photon and hadron rapidities from -2 to

2. In the left (right) panel, the trigger photon momentum is integrated from $10 < p_{T_\gamma} < 20$ GeV ($25 < p_{T_\gamma} < 50$ GeV). The uncertainty band comes from the fact that we have included a $\sim 25\%$ uncertainty in the magnitude of the energy loss in our jet quenching calculation. The behavior of I_{AA} follows from similar considerations for the relevant kinematics. It is also interesting to notice that for low z_T both $I_{AA}^{\gamma B}$ and $I_{AA}^{\gamma D}$ can be larger than unity in the chosen kinematic region.

It will be illuminating and important to measure such correlations for both light and heavy meson production in p+p and A+A collisions at RHIC and at the LHC.

IV. CONCLUSIONS

We studied photon-triggered light hadron and heavy meson production in both p+p and A+A collisions. We found that the energy loss approach that was successful in describing single hadron production in A+A reactions at RHIC could simultaneously describe the STAR and PHENIX experimentally extracted photon-triggered light hadron fragmentation functions. Using the same theoretical framework, we generalized our formalism to study photon-triggered heavy meson production. To take into account the heavy quark mass explicitly, we followed the so-called fixed-flavor-number scheme and derived the differential cross section for photon+away-side heavy meson. We found that the nuclear modification of photon-tagged heavy meson fragmentation functions in A+A collision is very different from that of the photon-tagged light hadron fragmentation functions. This variance was determined to arise from the different shape of the decay probabilities for light partons into light hadrons and heavy quarks into heavy mesons, respectively. Comparing D and B-mesons, we predicted that the nuclear modification factor I_{AA} would be flatter for $\gamma+B$ production than the one for the $\gamma+D$ case. This is directly related to the different amount of energy lost by heavy quarks with different mass. Thus, the different shape of I_{AA} in $\gamma+h$, $\gamma+D$, and $\gamma+B$ productions can be a sensitive and quantitative probe of the strength of medium-induced parton energy loss. Finally, we made detailed predictions for both photon-triggered light and heavy meson at RHIC and at the LHC. We conclude by emphasizing once again that a comprehensive study of these new final-state channels will provide fresh insight into the details of the jet quenching mechanism.

ACKNOWLEDGMENTS

Note added: we recently became aware of the fact that F. Arleo, I. Schienbein and T. Stavreva are working on a similar problem by extending earlier work relevant to p+A collisions [43].

[1] M. Gyulassy and X. N. Wang, Nucl. Phys. B **420**, 583 (1994) [arXiv:nucl-th/9306003].
[2] R. Baier, Y. L. Dokshitzer, A. H. Mueller, S. Peigne and D. Schiff, Nucl. Phys. B **484**, 265 (1997) [arXiv:hep-ph/9608322].
[3] B. G. Zakharov, JETP Lett. **65**, 615 (1997) [arXiv:hep-ph/9704255].
[4] U. A. Wiedemann, Nucl. Phys. B **588**, 303 (2000) [arXiv:hep-ph/0005129].
[5] M. Gyulassy, P. Levai and I. Vitev, Nucl. Phys. B **594**, 371 (2001) [arXiv:nucl-th/0006010].
[6] X. N. Wang and X. f. Guo, Nucl. Phys. A **696**, 788 (2001) [arXiv:hep-ph/0102230].
[7] P. B. Arnold, G. D. Moore, L. G. Yaffe, JHEP **0206**, 030 (2002). [hep-ph/0204343].
[8] G. Ovanesyan, I. Vitev, [arXiv:1103.1074 [hep-ph]].
[9] D. d'Enterria, [arXiv:0902.2011 [nucl-ex]].
[10] K. Adcox *et al.* [PHENIX Collaboration], Phys. Rev. Lett. **88**, 022301 (2002) [arXiv:nucl-ex/0109003].
[11] C. Adler *et al.* [STAR Collaboration], Phys. Rev. Lett. **89**, 202301 (2002) [arXiv:nucl-ex/0206011].
[12] K. Aamodt *et al.* [ALICE Collaboration], Phys. Lett. B **696**, 30 (2011)
[13] C. Adler *et al.* [STAR Collaboration], Phys. Rev. Lett. **90**, 082302 (2003) [arXiv:nucl-ex/0210033].
[14] A. Adare *et al.* [The PHENIX Collaboration], Phys. Rev. Lett. **104**, 252301 (2010) [arXiv:1002.1077 [nucl-ex]].
[15] A. Adare *et al.* [PHENIX Collaboration], Phys. Rev. C **80**, 024908 (2009) [arXiv:0903.3399 [nucl-ex]].
[16] B. I. Abelev *et al.* [STAR Collaboration], Phys. Rev. C **82**, 034909 (2010) [arXiv:0912.1871 [nucl-ex]].
[17] S. Salur, Nucl. Phys. A **830**, 139C (2009) [arXiv:0907.4536 [nucl-ex]].
[18] G. Aad *et al.* [Atlas Collaboration], Phys. Rev. Lett. **105**, 252303 (2010) [arXiv:1011.6182 [hep-ex]].
[19] S. Chatrchyan *et al.* [CMS Collaboration], arXiv:1102.1957 [nucl-ex].
[20] See, for example: H. Z. Zhang, Z. B. Kang, B. W. Zhang and E. Wang, Eur. Phys. J. C **67**, 445 (2010) [arXiv:hep-ph/0609159]; I. Vitev and B. W. Zhang, Phys. Rev. Lett. **104**, 132001 (2010) [arXiv:0910.1090 [hep-ph]]; Y. He, I. Vitev and B. W. Zhang, arXiv:1105.2566 [hep-ph]; and the references therein.
[21] X. N. Wang, Z. Huang and I. Sarcevic, Phys. Rev. Lett. **77**, 231 (1996) [arXiv:hep-ph/9605213]; X. N. Wang and Z. Huang, Phys. Rev. C **55**, 3047 (1997) [arXiv:hep-ph/9701227].
[22] H. Zhang, J. F. Owens, E. Wang and X. N. Wang, Phys. Rev. Lett. **103**, 032302 (2009) [arXiv:0902.4000 [nucl-th]].
[23] G. Y. Qin, J. Ruppert, C. Gale, S. Jeon and G. D. Moore, Phys. Rev. C **80**, 054909 (2009) [arXiv:0906.3280 [hep-ph]].
[24] T. Renk, Phys. Rev. **C80**, 014901 (2009). [arXiv:0904.3806 [hep-ph]].
[25] Y. L. Dokshitzer and D. E. Kharzeev, Phys. Lett. B **519**, 199 (2001) [arXiv:hep-ph/0106202].
[26] S. Wicks, W. Horowitz, M. Djordjevic and M. Gyulassy, Nucl. Phys. A **784**, 426 (2007) [arXiv:nucl-th/0512076].
[27] A. Adil and I. Vitev, Phys. Lett. B **649**, 139 (2007) [arXiv:hep-ph/0611109].
[28] R. Sharma, I. Vitev and B. W. Zhang, Phys. Rev. C **80**, 054902 (2009) [arXiv:0904.0032 [hep-ph]].
[29] J. F. Owens, Rev. Mod. Phys. **59**, 465 (1987).
[30] S. Frixione, M. L. Mangano, P. Nason and G. Ridolfi, Phys. Lett. B **348**, 633 (1995) [arXiv:hep-ph/9412348].
[31] S. Frixione, P. Nason and G. Ridolfi, Nucl. Phys. B **454**, 3 (1995) [arXiv:hep-ph/9506226]; and earlier references given there.
[32] M. Stratmann and W. Vogelsang, Phys. Rev. D **52**, 1535 (1995).
[33] E. L. Berger and L. E. Gordon, Phys. Rev. D **54**, 2279 (1996) [arXiv:hep-ph/9512343].
[34] B. Bailey, E. L. Berger and L. E. Gordon, Phys. Rev. D **54**, 1896 (1996) [arXiv:hep-ph/9602373].
[35] T. P. Stavreva and J. F. Owens, Phys. Rev. D **79**, 054017 (2009) [arXiv:0901.3791 [hep-ph]].
[36] R. K. Ellis and Z. Kunszt, Nucl. Phys. B **303**, 653 (1988).
[37] See, for example: I. Vitev and M. Gyulassy, Phys. Rev. Lett. **89**, 252301 (2002) [arXiv:hep-ph/0209161]; X. N. Wang, Phys. Rev. C **70**, 031901 (2004) [arXiv:nucl-th/0405029]; A. Adil and M. Gyulassy, Phys. Lett. B **602**, 52 (2004) [arXiv:nucl-th/0405036].
[38] M. Gyulassy, P. Levai and I. Vitev, Phys. Rev. Lett. **85**, 5535 (2000) [arXiv:nucl-th/0005032].
[39] I. Vitev, Phys. Rev. C **75**, 064906 (2007) [arXiv:hep-ph/0703002].
[40] R. B. Neufeld, I. Vitev and B. W. Zhang, Phys. Rev. C **83**, 034902 (2011) [arXiv:1006.2389 [hep-ph]].
[41] J. Pumplin, D. R. Stump, J. Huston, H. L. Lai, P. M. Nadolsky and W. K. Tung, JHEP **0207**, 012 (2002) [arXiv:hep-ph/0201195].
[42] D. de Florian, R. Sassot and M. Stratmann, Phys. Rev. D **75**, 114010 (2007) [arXiv:hep-ph/0703242].
[43] T. Stavreva, I. Schienbein, F. Arleo, K. Kovarik, F. Olness, J. Y. Yu, J. F. Owens, JHEP **1101**, 152 (2011). [arXiv:1012.1178 [hep-ph]].